JACS
JOURNAL OF THE AMERICAN CHEMICAL SOCIETY

Communication

pubs.acs.org/JACS

Two-Photon Spectroscopy as a New Sensitive Method for Determining the DNA Binding Mode of Fluorescent Nuclear Dyes

Phi H. Doan,[†] Demar R. G. Pitter,[‡] Andrea Kocher,[†] James N. Wilson,[‡] and Theodore Goodson, III*[,†]

[†]Department of Chemistry, University of Michigan, Ann Arbor, Michigan 48109, United States

[‡]Department of Chemistry, University of Miami, Coral Gables, Florida 33146, United States

Supporting Information

ABSTRACT: A new optical strategy to determine the binding modes (intercalation vs groove binding) of small fluorescent organic molecules with calf thymus DNA was developed using two-photon absorption (TPA) spectroscopy. Two-photon excited emission was utilized to investigate a series of fluorescent nuclear dyes. The results show that TPA cross-sections are able to differentiate the fine details between the DNA binding modes. Groove binding molecules exhibit an enhanced TPA cross-section due to the DNA electric field induced enhancement of the transition dipole moment, while intercalative binding molecules exhibit a decrease in the TPA cross-section. Remarkably, the TPA cross-section of 4,6-bis(4-(4-methylpiperazin-1-yl)phenyl) pyrimidine is significantly enhanced (13.6-fold) upon binding with DNA. The sensitivity of our TPA methodology is compared to circular dichroism spectroscopy. TPA demonstrates superior sensitivity by more than an order of magnitude at low DNA concentrations. This methodology can be utilized to probe DNA interactions with other external molecules such as proteins, enzymes, and drugs.

Fluorescent molecular nuclear dyes have been widely used in cellular biology with potential applications in forensic, diagnostic, and bioanalytical analysis.[1] Fluorophores that display enhanced fluorescence upon binding with DNA have been utilized in fluorescence microscopy as well as quantifying nucleic acids in gel electrophoresis and flow cytometry.[2] The binding interactions of external molecules with DNA often result in a significant change in their properties, which has an important impact on physiological functions.[3] Thus, the binding mode is a crucial parameter for drugs targeted at DNA. DNA binding molecules interact with DNA through intercalation or groove binding as represented in Figure 1A and 1B, respectively. Common effects of DNA intercalative drugs inhibit cell growth, cell transformation, and cell death, which have applications as antitumor, antibacterial, and antiparasitic agents.[4] Several DNA groove binding drugs act by interfering with cellular processes, which target enzyme and protein access to DNA.[5] The mechanism of binding is key to the performance of both DNA-targeted therapies and fluorescent probes. While basic design principles are proposed, the binding modes of many dyes cannot be unambiguously assigned based on either their structure or through the use of many well-established spectroscopic techniques. Therefore, distinguishing between an intercalator and groove binder is critical for the design of DNA-targeted drugs and fluorescent probes.

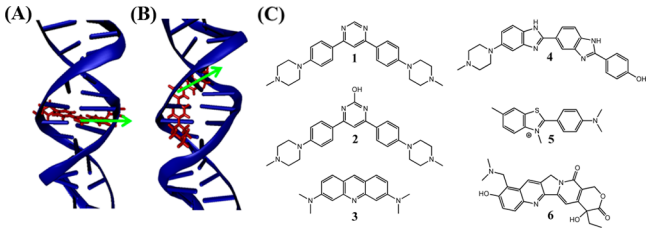

Figure 1. (A) Intercalative and (B) groove binding modes. Orientation of the $S_0 \rightarrow S_1$ transition dipole is shown in green. (C) Chemical structures of 4,6-bis(4-(4-methylpiperazin-1-yl)phenyl) pyrimidine (**1**), 4,6-bis(4-(4-methylpiperazin-1-yl)phenyl) pyrimidin-2-ol (**2**), acridine orange (**3**), Hoechst 33258 (**4**), thioflavin t (**5**), and topotecan (**6**).

Qualitative methods have been employed to elucidate the binding modes of external molecules to DNA.[3] However, a combination of select methods must be used to determine the DNA binding mode with certainty.[6] New methodologies, such as two-photon absorption (TPA), can provide a powerful tool to examine the photophysical properties of fluorescent organic molecules in biological systems.[7] TPA is a nonlinear technique that can be used with high sensitivity to understand the changes in the chromophore DNA binding environment, charge transfer character, and excited-dipoles.[8] We present the first results of two-photon spectroscopy to diagnose the DNA binding modes of small fluorescent molecules with calf thymus DNA (ctDNA). The change in the TPA cross-section (δ) was examined to assess the binding mode based on the DNA electric field induced perturbation of the dye's transition dipole. A series of dyes (Figure 1C) were investigated to demonstrate our methodology. These fluorophores illustrate a general scaffold for DNA binding dyes, which include linear, crescent, or planar structural motifs.

Reaction of 4,6-bis(4-fluorophenyl)pyrimidine[9] with *N*-methylpiperazine by nucleophilic aromatic substitution afforded **1** with an overall yield of 41%. The Biginelli reaction of 4-(4-methyl-1-piperazinyl) benzaldehyde, 4-(4-methyl-1-piperazinyl) acetophenone, and urea yielded **2**.[10] The steady-state absorption spectra, emission spectra, quantum yield, and characterization data can be found in the Supporting Information.

It has been shown that the local electric fields have an influence on the TPA cross-section.[11] The TPA cross-sections of triphenylamines with *N*-methyl benzimidazolium moiety termi-

Received: December 19, 2014
Published: June 29, 2015

DOI: 10.1021/jacs.5b02674
J. Am. Chem. Soc. 2015, 137, 9198−9201

nated branched dyes have been investigated, and it was reported that the TPA cross-section enhances about 10-fold upon groove binding with DNA.[12,13] We also present a TPA cross-section enhancement for the characterization of groove binding molecules similar to Dumat et al.[12] However, we attribute the TPA cross-section change to the DNA electric field influence on the dipole of the binding molecule. The change in the TPA cross-section is analyzed to determine the DNA binding mode based on the orientation of the binding agent relative to the DNA helical axis. A groove binding molecule will have a dipole oriented more parallel to the DNA electric field resulting in an enhanced TPA cross-section upon binding. Contrarily, an intercalating molecule will have a dipole aligned more perpendicular to the DNA electric field leading to a decreased TPA cross-section upon binding. A groove binding molecule will exhibit an increased induced dipole, while an intercalating molecule will have a decreased induced dipole due to the DNA electric field perturbation. It was reported that DNA has the capacity to accumulate an electric field.[14] Additionally, it has been shown that tethered dsDNA monomers, dimers, and trimers exhibit different extension lengths when an external electric field is applied.[15] This suggests that the electric field (dipole) of DNA changes with increasing DNA concentration for a given system. Therefore, we expect a change in the TPA cross-section of the dye upon binding with DNA.

To demonstrate our methodology, **3** and **4** were used as standards. It is important to note that **3** has been reported as a intercalator,[16] and **4** has been reported as a groove binder.[17] The TPA cross-sections were measured utilizing the two-photon excited fluorescence (TPEF) method.[18] For **3**, a decrease in the TPA cross-section was observed as the DNA concentration was increased (Figure 2A). This can be rationalized by the

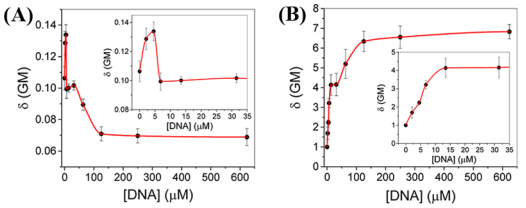

Figure 2. TPA cross-section of (A) **3** and (B) **4** plotted as a function of DNA (base pairs) concentration with [dye] = 5 μM. Inset graph: enlargement at low DNA concentration. Results are the mean ± SD (n = 3). The red line is to guide the eye.

orientation of **3** upon intercalating to DNA. The dipole of **3** is oriented more perpendicular to the DNA electric field (parallel to the bases) leading to a reduction in the induced dipole. The decreasing trend is evident of a DNA intercalative binding mode resulting in lengthening and unwinding of the DNA helix.[6] Important driving factors for intercalation are π-stacking, dispersive interaction, dipole−dipole interaction, and electrostatic factors with the aromatic nucleobases in DNA.[19] The TPA cross-section was also measured in the presence of [poly(dG-dC)]$_2$ (see Supporting Information). The results confirm that the decreasing TPA cross-section trend is directly related to **3** intercalating at GC base pairs. It was previously reported that **3** intercalates at GC-rich sequences,[20] which corresponds with our results. Interestingly, the TPA cross-section increased from 0.11 to 0.13 GM when the DNA concentration was increased to 4 μM. This observation can be explained due to the dye−dye interactions at high dye-to-DNA ratios, which were also observed at 7 μM of DNA using circular dichroism (CD). The dyes form ordered aggregates at the surface of DNA[21] resulting in an enhanced dipole, which influences the TPA cross-section.

4 was investigated to demonstrate our methodology for a well-known groove binder. An increasing TPA cross-section trend was observed with increasing DNA concentrations (Figure 2B). A TPA cross-section enhancement of 6.9-fold was noted upon binding with DNA. The dipole of **4** is aligned more parallel to the DNA electric field when bound, resulting in an enhanced TPA cross-section. The increasing trend indicates a DNA groove binding mode, which is characterized by little to no perturbation of the DNA structure.[22] Groove binding molecules require conformational flexibility that allows the molecule to fit into the groove and functional groups that interact with the nucleobases with minimal steric hindrance.[3] The TPA cross-section of **4** was measured in the presence of [poly(dA-dT)]$_2$ (see Supporting Information). A TPA cross-section enhancement of 7.4-fold was observed upon binding at AT base pairs. The findings confirm that the TPA cross-section enhancement is directly related to **4** groove binding at AT-rich sequences. **4** was reported to groove bind along AT-rich sequences while occupying four base pairs[23] through van der Waals and hydrogen bonding interactions.[24]

CD measurements were applied to compare with the TPA analysis. Positive and negative induced circular dichroism (ICD) signals were observed near 480 and 465 nm, respectively, for **3** (see Supporting Information). The positive band is due to the interaction between the transition dipoles of two or more ordered dyes and reduces when DNA concentrations are increased.[21] The negative ICD signal near 465 nm is attributed to the intercalated dye.[25] Contrarily, a strong positive ICD signal was observed at approximately 360 nm for the interaction of **4** with DNA (see Supporting Information). The positive band is ascribed to **4** groove binding with DNA.[26]

TPA was employed to study the binding mode of thioflavin t (**5**). It was previously reported that **5** intercalates with dsDNA.[27] **5** undergoes a twisted internal charge-transfer (TICT), which is responsible for the quenched fluorescence in the absence of DNA. When bound with DNA, the internal rotation of the dye is restricted due to steric hindrance resulting in enhanced fluorescence.[28] Presented in Figure 3A, the decreasing trend is

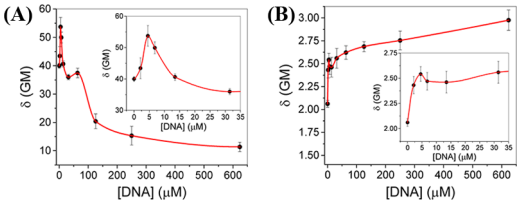

Figure 3. TPA cross-section of (A) **5** and (B) **6** plotted as a function of DNA (base pairs) concentration with [dye] = 5 μM. Inset graph: enlargement at low DNA concentration. Results are the mean ± SD (n = 3). The red line is to guide the eye.

indicative of an intercalative binding mode. This suggests that the dipole of **5** is oriented more perpendicular with the DNA electric field upon binding. **5** had a TPA cross-section of 40.0 GM in the absence of DNA. The TPA cross-section decreased to 11.4 GM at 624 μM of DNA. The decrease in the TPA cross-section can be attributed to the DNA electric field induced perturbation of the dye's transition dipole rather than the conformational change of the dye upon intercalation since **1**, **2**, and **4** undergo a conformational change upon groove binding. Similar to **3**, the TPA cross-section increased at low DNA concentrations. The

DOI: 10.1021/jacs.5b02674
J. Am. Chem. Soc. 2015, 137, 9198−9201

TPA cross-section increased to 53.7 GM at 4 μM of DNA, which can be attributed to the formation of dimers that bind at the DNA grooves under excess dye conditions.[29] CD was used to compare with the TPA experiments. However, an ICD signal was not detected at our experimental conditions (see Supporting Information). This demonstrates that TPA is more sensitive at low dye concentrations as compared to CD. Bathochromic shifts of 8 and 48 nm were observed in the absorption and emission spectra, respectively, at 624 μM of DNA, indicating the dye is bound with DNA (see Supporting Information).

The binding mode of topotecan (**6**), a clinically approved anticancer drug, was investigated using TPA. There has been controversy regarding the binding mode of **6**. The binding mechanism is of interest because therapeutic importance can be improved. Yang et al.[30] reported an intercalating binding mode in the absence of topoisomerase I. However, Streltsov et al.[31] and Joshi et al.[32] concluded that **6** binds to DNA through a groove binding mechanism. Our TPA analysis suggests that **6** groove binds with DNA, as shown in Figure 3B. The TPA cross-section enhancement can be attributed to **6** groove binding at GC-rich sequences.[31,32] Quenching in both the steady-state and two-photon excited emission was observed (see Supporting Information). This can be ascribed to the photoinduced electron transfer (PET) between the drug and DNA nucleobases.[32] A TPA cross-section enhancement of 1.5-fold was noted upon binding with DNA. The low enhancement can be attributed to the orientation of the binding agent relative to the DNA helical axis. **6** was reported to be oriented nearly 55° to the DNA helical axis, which is approximate to a groove binder (<55°) but less than a classical intercalator (62−76°).[31,32] Comparatively, **4** had a TPA cross-section enhancement of 6.9-fold with a 45° angle of orientation.[33] The difference in the TPA cross-section enhancement at low and high DNA concentrations can be ascribed to the DNA electric field induced enhancement of the dye's transition dipole. The low TPA cross-section enhancement suggests that the binding angle of topotecan is between an intercalator and groove binder. A larger TPA cross-section enhancement is expected if the dipole of the binding molecule is oriented more parallel with the DNA electric field.

The binding mode of **1** was studied utilizing TPA and CD. The TPA cross-section of the unbound dye was 2.1 GM. Shown in Figure 4A, the TPA cross-section increased to 28.7 GM at 624 μM of DNA. A significant TPA cross-section enhancement of 13.6-fold was observed upon binding with DNA, which was the largest enhancement noted. The TPA cross-section enhancement indicates that **1** undergoes a groove binding mechanism in the presence of DNA. The crescent shape of **1** allows the molecule to groove bind at AT-rich sequences. CD was used to

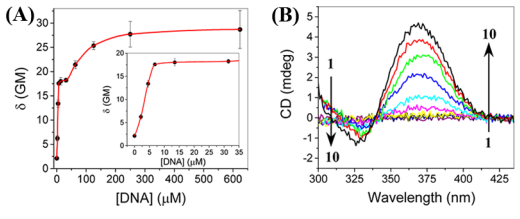

Figure 4. (A) TPA cross-section of **1** (5 μM) plotted as a function of DNA (base pairs) concentration. Inset graph: enlargement at low DNA concentration. Results are the mean ± SD (n = 3). The red line is to guide the eye. (B) CD spectra at different DNA concentrations. 1 → 10 represents DNA (base pairs) concentrations 0, 2, 4, 7, 14, 32, 63, 125, 250, and 624 μM, respectively.

investigate the system. **1** exhibits a positive ICD signal near 370 nm in the presence of DNA, which is consistent of a groove binding mode (Figure 4B). The positive band corresponds to the $S_0 \rightarrow S_1$ transition, which suggests that the transition dipole of **1** is oriented along the groove.[34] Interestingly, a weak negative band is observed near 325 nm at 32 μM of DNA or greater. The bisignate ICD signal is attributed to the formation of dimers at the surface or in the groove of DNA.[35] In agreement with CD, the TPA cross-section enhancement indicates that the transition dipole of **1** is oriented more parallel to the DNA electric field.

TPA and CD were employed to investigate the binding mode of **2**. Presented in Figure 5A, the TPA cross-section is plotted as a

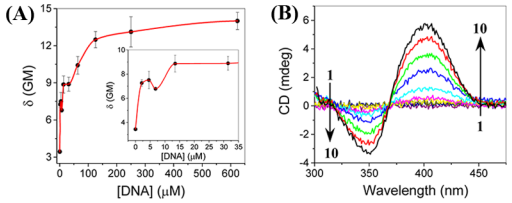

Figure 5. (A) TPA cross-section of **2** (5 μM) plotted as a function of DNA (base pairs) concentration. Inset graph: enlargement at low DNA concentration. Results are the mean ± SD (n = 3). The red line is to guide the eye. (B) CD spectra at different DNA concentrations. 1 → 10 represents DNA (base pairs) concentrations 0, 2, 4, 7, 14, 32, 63, 125, 250, and 624 μM, respectively.

function of DNA concentration. The TPA cross-section increased from 3.4 to 14.0 GM from 0 to 624 μM of DNA. A TPA cross-section enhancement of 4.1-fold was observed. Compared with **1**, this suggests that a larger TPA cross-section enhancement is noted when a less electron withdrawing heterocyclic central core is incorporated into the donor−acceptor−donor π-system. In addition, the hydroxyl substituent from **2** may interact with the DNA nucleobases and surrounding water molecules resulting in a lower TPA cross-section enhancement.[36] The increasing trend indicates that **2** interacts with DNA though a groove binding mechanism. CD was used to examine the binding mode of **2** (Figure 5B). A positive ICD signal was recorded in the presence of DNA near 400 nm, which corresponds to the $S_0 \rightarrow S_1$ transition. The negative band at approximately 350 nm corresponds to the $S_0 \rightarrow S_2$ transition. **2** was previously reported to groove bind with DNA using linear dichroism (LD),[10] which agrees with the TPA analysis. Additionally, it was shown that **2** interacts with DNA through hydrogen bonding interactions at the AT base pairs, occupying three base pairs. However, the fluorescence is nearly quenched from GC sequences, which is most likely due to the PET from guanine to the excited chromophore.[37]

A direct comparison of TPA and CD demonstrates superior sensitivity compared to CD. It is important to note an ICD signal was not observed for **5** and **6**; however, a change was detected utilizing TPA. This indicates that our method has superior sensitivity at low dye and DNA concentrations. An ICD signal was not observed at DNA concentrations less than 7 μM for **1**−**3**. However, an ICD signal was detected at 4 μM of DNA for **4**. TPA detected a significant environmental change in the presence of 2 μM of DNA for all compounds, which demonstrates that the methodology has potential use at biologically relevant concentrations while avoiding problems with background absorption of common buffers.[38] For example, the TPA cross-section increased from 2.1 to 6.2 GM when the DNA concentration was increased to 2 μM for **1**. The findings are significant, as it suggests that two-

DOI: 10.1021/jacs.5b02674
J. Am. Chem. Soc. 2015, 137, 9198−9201

photon spectroscopy can provide detailed information at dilute concentrations of DNA and differentiate between the DNA binding modes of external molecules, which are inaccessible with single-photon excited fluorescence. Furthermore, two-photon excitation microscopy (TPEM) can be used for cellular studies. Since the TPA process is quadratically intensity dependent, TPEM can provide superior spatial resolution with reduced photobleaching and photodamage as well as autofluorescence for bioimaging at low concentrations.

In conclusion, we developed a new highly sensitive methodology to diagnose the DNA binding mode of external molecules. This report is the first example that applied TPA cross-section changes to determine the DNA binding mode of fluorescent nuclear dyes and DNA-targeted drugs. The TPA cross-sections of intercalating and groove binding dyes are influenced by the electric field of the DNA backbone upon binding. An increasing TPA cross-section trend is indicative of a groove binding mode, while a decreasing TPA cross-section trend suggests an intercalative binding mode. A comparison of our TPA studies with CD demonstrates that TPA exhibits superior sensitivity at DNA concentrations of 4 μM and lower by more than an order of magnitude. This work may facilitate the biological studies of DNA interactions with other external molecules as well as applications for bioimaging.

■ ASSOCIATED CONTENT

Supporting Information

Detailed experimental procedures, synthesis of chromophores, fluorescence quantum yields, CD, absorption, and emission spectra. The Supporting Information is available free of charge on the ACS Publications website at DOI: 10.1021/jacs.5b02674.

■ AUTHOR INFORMATION

Corresponding Author

*tgoodson@umich.edu

Notes

The authors declare no competing financial interest.

■ ACKNOWLEDGMENTS

T.G.III acknowledges the National Science Foundation for support (F019767-057852). J.W. acknowledges the support from the Florida Department of Health Bankhead-Coley New Investigator Research Program (3BN08).

■ REFERENCES

(1) Wang, J. *Nucleic Acids Res.* **2008**, *28*, 3011.
(2) Benvin, A. L.; Creeger, Y.; Fisher, G. W.; Ballou, B.; Waggoner, A. S.; Armitage, B. A. *J. Am. Chem. Soc.* **2007**, *129*, 2025.
(3) Ihmels, H.; Otto, D. *Top Curr. Chem.* **2005**, *258*, 161.
(4) Berman, H. M.; Young, P. R. *Annu. Rev. Biophys. Bioeng.* **1981**, *10*, 87.
(5) Mukherjee, A.; Lavery, R.; Bagchi, B.; Hynes, J. T. *J. Am. Chem. Soc.* **2008**, *130*, 9747.
(6) Suh, D.; Chaires, J. B. *Bioorg. Med. Chem.* **1995**, *3*, 723.
(7) (a) Clark, T. B.; Ziółkowski, M.; Schatz, G. C.; Goodson, T., III *J. Phys. Chem. B* **2014**, *118*, 2351. (b) McLean, A. M.; Socher, E.; Varnavski, O.; Clark, T. B.; Imperiali, B.; Goodson, T., III *J. Phys. Chem. B* **2013**, *117*, 15935. (c) Wang, Y.; Clark, T. B.; Goodson, T. *J. Phys. Chem. B* **2010**, *114*, 7112.
(8) (a) Wang, Y.; He, G. S.; Prasad, P. N.; Goodson, T. *J. Am. Chem. Soc.* **2005**, *127*, 10128. (b) Flynn, D. C.; Ramakrishna, G.; Yang, H. B.; Northrop, B. H.; Stang, P. J.; Goodson, T., III *J. Am. Chem. Soc.* **2010**, *132*, 1348. (c) Bhaskar, A.; Guda, R.; Haley, M. M.; Goodson, T., III *J. Am. Chem. Soc.* **2006**, *128*, 13972.
(9) (a) Wheelhouse, R. T.; Jennings, S. A.; Phillips, V. A.; Pletsas, D.; Murphy, P. M.; Garbett, N. C.; Chaires, J. B.; Jenkins, T. C. *J. Med. Chem.* **2006**, *49*, 5187. (b) Qing, F.-L.; Wang, R.; Li, B.; Zheng, X.; Meng, W.-D. *J. Fluorine Chem.* **2003**, *120*, 21.
(10) Pitter, D. R.; Wigenius, J.; Brown, A. S.; Baker, J. D.; Westerlund, F.; Wilson, J. N. *Org. Lett.* **2013**, *15*, 1330.
(11) (a) Drobizhev, M.; Makarov, N. S.; Tillo, S. E.; Hughes, T. E.; Rebane, A. *Nat. Methods* **2011**, *8*, 393. (b) Drobizhev, M.; Tillo, S.; Makarov, N. S.; Hughes, T. E.; Rebane, A. *J. Phys. Chem. B* **2009**, *113*, 12860. (c) Bairu, S.; Ramakrishna, G. *J. Phys. Chem. B* **2013**, *117*, 10484.
(12) Dumat, B.; Bordeau, G.; Faurel-Paul, E.; Mahuteau-Betzer, F.; Saettel, N.; Metge, G.; Fiorini-Debuisschert, C.; Charra, F.; Teulade-Fichou, M.-P. *J. Am. Chem. Soc.* **2013**, *135*, 12697.
(13) Allain, C.; Schmidt, F.; Lartia, R.; Bordeau, G.; Fiorini-Debuisschert, C.; Charra, F.; Tauc, P.; Teulade-Fichou, M.-P. *ChemBioChem* **2007**, *8*, 424.
(14) (a) Takashima, S. *J. Mol. Biol.* **1963**, *7*, 455. (b) Saxena, V. K.; Van Zandt, L. L. *Phys. Rev. A: At., Mol., Opt. Phys.* **1992**, *45*, 7610.
(15) (a) Stigter, D. *Biophys. Chem.* **2002**, *101-102*, 447. (b) Stigter, D.; Bustamante, C. *Biophys. J.* **1998**, *75*, 1197. (c) Ferree, S.; Blanch, H. W. *Biophys. J.* **2003**, *85*, 2539.
(16) Armstrong, R. W.; Kurucsev, T.; Strauss, U. P. *J. Am. Chem. Soc.* **1970**, *92*, 3174.
(17) Furse, K. E.; Corcelli, S. A. *J. Am. Chem. Soc.* **2008**, *130*, 13103.
(18) Xu, C.; Webb, W. *J. Opt. Soc. Am. B* **1996**, *13*, 481.
(19) Reynisson, J.; Schuster, G. B.; Howerton, S. B.; Williams, L. D.; Barnett, R. N.; Cleveland, C. L.; Landman, U.; Harrit, N.; Chaires, J. B. *J. Am. Chem. Soc.* **2003**, *125*, 2072.
(20) Nafisi, S.; Saboury, A. A.; Keramat, N.; Neault, J. F.; Tajmir-Riahi, H. A. *J. Mol. Struct.* **2007**, *827*, 35.
(21) Zama, M.; Ichimura, S. *Biopolymers* **1970**, *9*, 53.
(22) Mallena, S.; Lee, M. P.; Bailly, C.; Neidle, S.; Kumar, A.; Boykin, D. W.; Wilson, W. D. *J. Am. Chem. Soc.* **2004**, *126*, 13659.
(23) Fornander, L. H.; Wu, L.; Billeter, M.; Lincoln, P.; Nordén, B. *J. Phys. Chem. B* **2013**, *117*, 5820.
(24) Wan, K. X.; Shibue, T.; Gross, M. L. *J. Am. Chem. Soc.* **2000**, *122*, 300.
(25) Mason, S. F.; McCaffery, A. J. *Nature* **1964**, *204*, 468.
(26) Willis, B.; Arya, D. P. *Biochemistry* **2006**, *45*, 10217.
(27) (a) Cañete, M.; Villanueva, A.; Juarranz, A.; Stockert, J. C. *Cell Mol. Biol.* **1987**, *33*, 191. (b) Zsila, F. *Int. J. Biol. Macromol.* **2015**, *72*, 1034. (c) Murudkar, S.; Mora, A. K.; Jakka, S.; Singh, P. K.; Nath, S. *J. Photochem. Photobiol., A* **2014**, *295*, 17.
(28) Stsiapura, V. I.; Maskevich, A. A.; Kuzmitsky, V. A.; Turoverov, K. K.; Kuznetsova, I. M. *J. Phys. Chem. A* **2007**, *111*, 4829.
(29) Biancardi, A.; Biver, T.; Burgalassi, A.; Mattonai, M.; Secco, F.; Venturini, M. *Phys. Chem. Chem. Phys.* **2014**, *16*, 20061.
(30) Yang, D.; Strode, J. T.; Spielmann, H. P.; Wang, A. H. J.; Burke, T. G. *J. Am. Chem. Soc.* **1998**, *120*, 2979.
(31) Streltsov, S.; Sukhanova, A.; Mikheikin, A.; Grokhovsky, A.; Zhuze, A.; Kudelina, I.; Mochalov, L.; Oleinikov, V.; Jardillier, J.-C.; Nabiev, I. *J. Phys. Chem. B* **2001**, *105*, 9643.
(32) Joshi, H.; Sengupta, A.; Gavvala, K.; Hazra, P. *RSC Adv.* **2014**, *4*, 1015.
(33) Moon, J. H.; Kim, S. K.; Sehlstedt, U.; Rodger, A.; Norden, B. *Biopolymers* **1996**, *38*, 593.
(34) Wilson, W. D.; Tanious, F. A.; Ding, D.; Kumar, A.; Boykin, D. W.; Colson, P.; Houssier, C.; Bailly, C. *J. Am. Chem. Soc.* **1998**, *120*, 10310.
(35) Seifert, J.; Connor, R.; Kushon, S. A.; Wang, M.; Armitage, B. A. *J. Am. Chem. Soc.* **1999**, *121*, 2987.
(36) Liu, Z.; Shao, P.; Huang, Z.; Liu, B.; Chen, T.; Qin, J. *Chem. Commun.* **2008**, *19*, 2260.
(37) Wilson, J. N.; Wigenius, J.; Pitter, D. R.; Qiu, Y.; Abrahamsson, M.; Westerlund, F. *J. Phys. Chem. B* **2013**, *117*, 12000.
(38) Greenfield, N. J. *Nat. Protoc.* **2007**, *1*, 2876.

DOI: 10.1021/jacs.5b02674
J. Am. Chem. Soc. 2015, 137, 9198−9201